A novel method for effective sodium ion implantation into silicon

Qiu Yuan Lu and Paul K. Chu[a)]
Department of Physics and Materials Science, City University of Hong Kong, Tat Chee Avenue, Kowloon, Hong Kong

(Received 29 May 2012; accepted 5 July 2012; published online 27 July 2012)

Although sodium ion implantation is useful to the surface modification of biomaterials and nano-electronic materials, it is a challenging to conduct effective sodium implantation by traditional implantation methods due to its high chemical reactivity. In this paper, we present a novel method by coupling a Na dispenser with plasma immersion ion implantation and radio frequency discharge. X-ray photoelectron spectroscopy (XPS) depth profiling reveals that sodium is effectively implanted into a silicon wafer using this apparatus. The Na 1*s* XPS spectra disclose Na_2O–SiO_2 bonds and the implantation effects are confirmed by tapping mode atomic force microscopy. Our setup provides a feasible way to conduct sodium ion implantation effectively. © *2012 American Institute of Physics*. [http://dx.doi.org/10.1063/1.4738663]

I. INTRODUCTION

Recently, the element sodium has attracted more attention in materials modification, especially biomaterials[1–5] and nano-electronic materials.[6–9] For instance, nickel titanium (NiTi) shape memory alloys are used in many biomedical applications including actuators, orthodontic arch wires, and cardiovascular stents due to the shape memory effect.[10] However, wider clinical applications have been hampered by the high toxic nickel content. While oxygen plasma immersion ion implantation (PIII) has been applied to increase the corrosion resistance of NiTi alloys and mitigate Ni release,[11] oxygen PIII treatment is not able to enhance the bioactivity of the materials. Therefore, some researchers have proposed the combined use of sodium and oxygen PIII to enhance the bioactivity and corrosion resistance of NiTi alloys.[5] As another example, ZnO-based semiconductors are uniquely suited for high efficiency light emission diodes due to the high exciton binding energy of 60 meV and large band gap of 3.37 eV at room temperature, but the main bottleneck the difficulty to fabricate stable p-type ZnO. The search for a good p-type dopant has received worldwide attention and sodium doping may provide the needed p-type behavior.[8] However, it is challenging to conduct effective sodium ion implantation by traditional implantation methods because sodium is chemically very reactive. Besides, its low melting point makes high-temperature means dangerous and infeasible. In this work, a novel setup and method are proposed to conduct sodium ion implantation.

II. DESIGN PRINCIPLE AND HARDWARE

The experimental setup is described in Fig. 1. Sodium particles are vented out when the activation current is applied to the Na dispenser™. The inductively coupled plasma antenna is located below the evaporation chamber and nitrogen is bled in to sustain the radio frequency (RF) discharge. Following ionization, the Na ions are implanted into the samples which are subjected to a negative high voltage. The apparatus is installed inside the vacuum chamber of the automated multi-purpose plasma processing system with the exception of the direct current (dc) and RF power supplies. The auxiliary gas (nitrogen) is fed into the evaporation chamber through the grounded gas inlet tube and the Na dispenser is heated by the dc power supply. According to the Handbook of Alkali Metal Dispensers,[12] the practical range of current is from 4.5 to 7.5 A. In our experiments, the current of the dc power supply is fixed at 7 A. Since the resistance of the dispenser fluctuates a little with temperature, the voltage varies from 3.2 to 3.4 V. The spiral antenna is connected to the RF power supply by copper wires wrapped by a polytetrafluoroethylene tube. The glass chamber serves two purposes. It keeps a high enough pressure to trigger the RF discharge at a low gas flux and minimize Na contamination to the system.

The experimental procedures are as follows. The power of the RF power supply was 200 W. The sample holder was biased by negative high voltage pulses with an amplitude of 20 kV, repetition frequency of 100 Hz, and pulse width of 50 μs. The RF power supply was turned on when nitrogen was fed into the evaporation chamber at a flow rate of $\sim$50 sccm. The dc power supply was turned on and the current was adjusted to 7 A. The discharge region turned from purple to light yellow after several seconds indicating that sodium was released from the Na dispenser and ionized by the RF discharge. Afterwards, the nitrogen flow rate was reduced to 20 sccm to maintain a pressure of 4.0×10^{-2} Pa. A typical implantation process lasted 1.5 h.

X-ray photoelectron spectroscopy (XPS, Physical electronics PHI 5802, MN) was employed to determine the in-depth distributions of Na, O, N, and Si. An aluminum x-ray source with a power of 350 W was used. The analysis area was $\sim$1 mm $\times$ 1 mm and the photoelectrons were detected at a take-off angle of 45°. The sputtering rate was about 3.96 nm/min. Tapping mode atomic force microscopy (AFM) was conducted to evaluate the surface morphology of a scanned area of 2×2 μm^2.

a)Author to whom correspondence should be addressed. Electronic mail: paul.chu@cityu.edu.hk. Tel.: +852-27887724. Fax: +852-27889549.

0034-6748/2012/83(7)/075116/3/$30.00

© 2012 American Institute of Physics

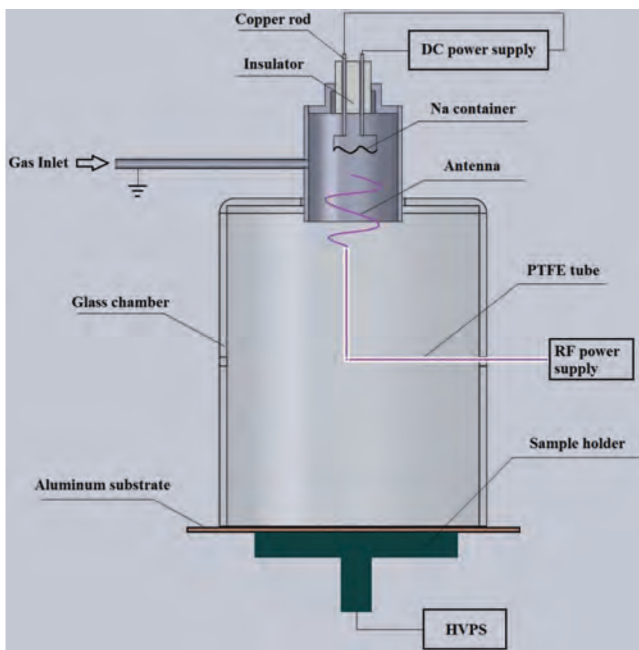

FIG. 1. Schematic diagram of the experimental setup (cross section). HVPS stands for the high voltage power supply.

III. RESULTS AND DISCUSSION

Figure 2 depicts the XPS elemental depth profiles of the silicon wafer after implanted. The quasi-Gaussian depth profiles of Na reveal that sodium has been implanted into the sample.[13,14] However, the projected range (R_p) of Na is smaller than that of roughly 40 nm calculated by Stopping and Range of Ions in Matter (SRIM) described in Figure 3.[15] It may be due to the chemical activity of sodium. Although the base vacuum in the implantation chamber is 4.2×10^{-4} Pa, there is residual oxygen in the chamber. When sodium is evaporated from the Na dispenser, most of it is oxidized to form Na_2O. Therefore, the net implantation energy of Na is less than that of elemental Na. Nitrogen is co-implanted and the depth profile consists of contributions from both N_2^+ and N^+. The shallower nitrogen peak than the calculated one may be due to sputtering during implantation. However, nitrogen co-implantation does not appear to affect the efficacy of Na implantation.[16] It may be because nitrogen is lighter than sodium and so knock-ons are not severe. In addition, no chemical bonds form between nitrogen and Na. It should be noted that nitrogen can be replaced by argon or another inert gas here, but our results suggest nitrogen which is more economical and adequate. The peak Na concentration is ∼10% which may be too low for some surface modification applications. The implantation fluence can be increased by using multiple dispensers simultaneously.

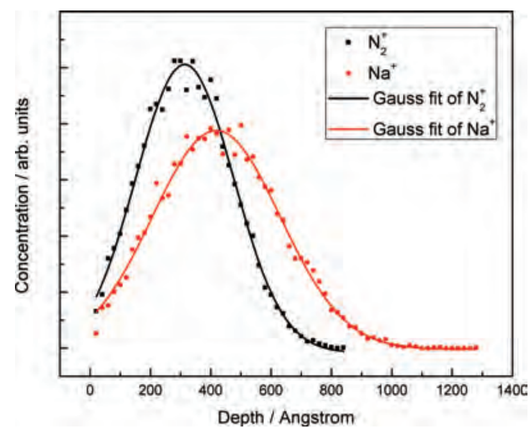

FIG. 3. SRIM depth profiles of Na^+ and N_2^+ (20 keV for Na^+ and 10 keV for N_2^+). The incident angle is 0° and no sputtering effect is taken into account in the calculation. The curves are the Gauss fits of the data points.

The binding energy of the Na 1*s* photoelectrons is between 1070 eV and 1075 eV.[16] The binding energy of series 2–10 in Fig. 4 increases gradually to 1071.8 eV, except series 1. According to Handbook of The Elements and Native Oxides, the binding energy of 1071.8 eV corresponds to the chemical state of $Na_2O–SiO_2$ suggesting that the implanted sodium is chemically bonded to silicon and oxygen. The bonding energy increases slowly because the ratio of SiO_2 to Na_2O increases with depth. Series 1 indicates the chemical state of the sample surface. It is different from the other series because NaOH can form on the surface of sodium-implanted

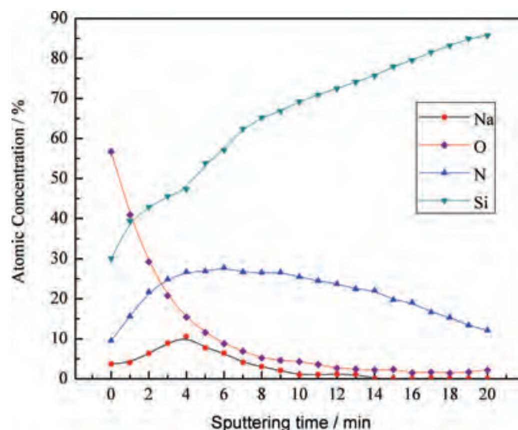

FIG. 2. Depth profiles acquired from the center of the samples after Na-PIII at −20 kV, 100 Hz, and 50 μs. Nitrogen used to sustain the discharge is co-implanted.

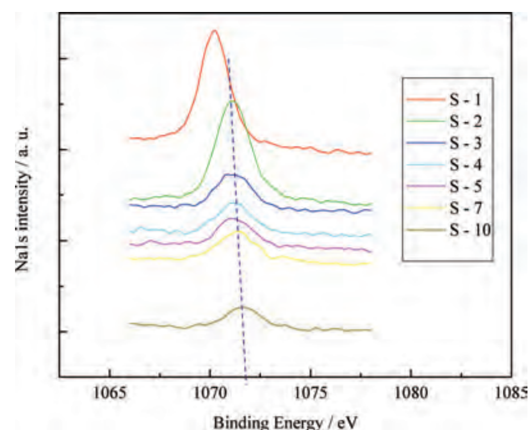

FIG. 4. Na 1*s* XPS spectra as a function of sputtered depths obtained from the Na-implanted silicon sample. S-1–S-10 are series 1–series 10 corresponding to increasing sputtering depths.

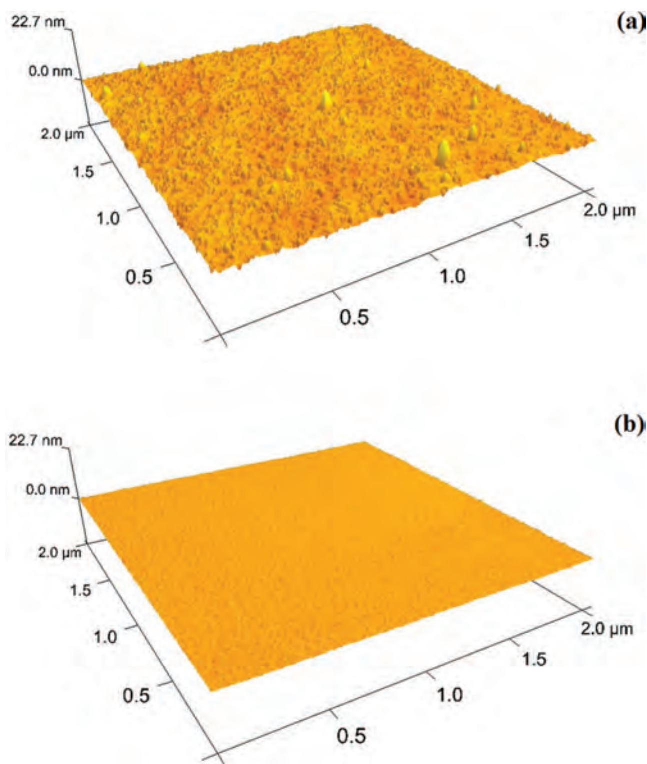

FIG. 5. AFM 3D images: (a) Sodium implanted silicon and (b) unimplanted silicon control.

silicon wafer upon exposure to residual air. The surface morphology of the sodium implanted silicon is examined by AFM and shown in Fig. 5(a). The surface roughness increases obviously compared to the control. The RMS roughness values of samples a and b are 0.757 nm and 0.154 nm, respectively. Large Na_2O and/or NaOH particles are observed from the surface. AFM shows indirectly that Na has been incorporated into the silicon sample.

IV. CONCLUSION

A method to conduct sodium ion implantation is proposed and demonstrated experimentally. A quasi-Gaussian Na depth profile is observed and Na ion implantation is not significantly influenced by co-implantation of nitrogen. The R_p of Na is smaller than that calculated theoretically due to molecular (Na_2O^+) implantation as confirmed by the Na 1s XPS spectra. It indicates that it is a key point to eliminate the residual oxygen to conduct more efficient sodium implantation. A larger ion implantation fluence can be achieved by using multiple Na dispensers simultaneously. Our setup provides a feasible way to conduct sodium ion implantation effectively.

ACKNOWLEDGMENTS

The work was financially supported by Hong Kong Research Grants Council Special Equipment Grant No. SEG_CityU05 and City University of Hong Kong Applied Research Grants No. 9667066.

[1] J. Baszkiewicz, D. Krupa, J. A. Kozubowski, B. Rajchel, M. Lewandowska-Szumiel, A. Barcz, J. W. Sobczak, A. Kosinski, and A. Chroscicka, J. Mater. Sci.: Mater. Med. **19**, 3081–3091 (2008).
[2] Y. L. Chan, S. L. Wu, X. M. Liu, P. K. Chu, K. W. K. Yeung, W. W. Lu, A. H. W. Ngan, K. D. K. Luk, D. Chan, and K. M. C. Cheung, Surf. Coat. Technol. **202**, 1308–1312 (2007).
[3] D. Krupa, J. Baszkiewicz, B. Rajchel, A. Barcz, J. W. Sobczak, and A. Bilinski, Vacuum **78**, 161–166 (2005).
[4] M. F. Maitz, R. W. Y. Poon, X. Y. Liu, M.-T. Pham, and P. K. Chu, Biomaterials **26**, 5465–5473 (2005).
[5] Y. L. Chan, K. W. K. Yeung, W. W. Lu, A. H. W. Ngan, K. D. K. Luk, D. Chan, S. L. Wu, X. M. Liu, P. K. Chu, and K. M. C. Cheung, Nucl. Instrum. Methods Phys. Res. B **257**, 687–691 (2007).
[6] V. M. Korol, Yu. Kudriavtsev, A. V. Zastavnoy, and S. A. Vedenyapin, Surf. Invest. X-Ray Synchrotron Neutron Tech. **3**, 292–297 (2009).
[7] P. T. Neuvonen, L. Vines, V. Venkatachalapathy, A. Zubiaga, F. Tuomisto, A. Hallen, B. G. Svensson, and A. Yu. Kuznetsov, Phys. Rev. B **84**, 205202 (2011).
[8] S. S. Lin, Z. Z. Ye, J. G. Lu, H. P. He, L. X. Chen, X. Q. Gu, J. Y. Huang, L. P. Zhu, and B. H. Zhao, J. Phys. D: Appl. Phys. **41**, 155114 (2008).
[9] E.-C. Lee and K. J. Chang, Phys. Rev. B **70**, 115210 (2004).
[10] T. Duerig, A. Pelton, and D. Stockel, Mater. Sci. Eng., A **149**, 273–275 (1999).
[11] R. W. Y. Poon, J. P. Y. Ho, X. Liu, C. Y. Chung, P. K. Chu, K. W. K. Yeung, W. W. Lu, and K. M. C. Cheung, Nucl. Instrum. Methods Phys. Res. B **237**, 411 (2005).
[12] See http://www.saesgetters.com/default.aspx?idPage=1584 for Alkali Metal Dispensers.
[13] A. Chen, J. Firmiss, and J. R. Conrad, J. Vac. Sci. Technol. B **12**, 918 (1994).
[14] J. R. Conrad, J. L. Radtke, R. A. Dodd, F. J. Worzala, and N. C. Tran, J. Appl. Phys. **62**, 4591 (1987).
[15] J. F. Ziegler, J. P. Biersack and U. Littmark, in *The Stopping and Range of Ions in Solids*, edited by J. F. Ziegler (Pergamon, New York, 1985).
[16] D. Labou and S. G. Neophytides, Solid State Ionics **177**, 971–977 (2006).